arXiv:1605.01252v1 [cond-mat.mtrl-sci] 4 May 2016

Random networks of carbon nanotubes optimized for transistor mass-production: multi-variable problem

M. Žeželj

School of Electrical Engineering, University of Belgrade, Bulevar kralja Aleksandra 73, 11120 Belgrade, Serbia
Scientific Computing Laboratory, Institute of Physics Belgrade, University of Belgrade, Pregrevica 118, 11080 Belgrade, Serbia

I. Stanković

Scientific Computing Laboratory, Institute of Physics Belgrade, University of Belgrade, Pregrevica 118, 11080 Belgrade, Serbia

E-mail: igor.stankovic@ipb.ac.rs

Abstract. Random networks of single-walled carbon nanotubes (CNTs) usually contain both metallic (m-CNTs) and semiconducting (s-CNTs) nanotubes with an approximate ratio of 1:2, which leads to a trade-off between on-conductance and on/off ratio. We demonstrate how the design problem can be solved with a realistic numerical approach. We determine CNT density, length, and channel dimensions for which CNT thin-film transistors (TFTs) simultaneously attain on-conductance higher than 1 μS and on/off ratio higher than 10^4. Fact that asymmetric systems have more pronounced finite-size scaling behavior than symmetric, enables us additional design freedom. A realisation probability of desired characteristics higher than 99% is obtained only with channel aspect length to width ratios $L_{\mathrm{CH}}/W_{\mathrm{CH}} < 1.2$ and normalized channel size $L_{\mathrm{CH}}W_{\mathrm{CH}}/l_{\mathrm{CNT}}^2 > 250$ for a range of CNT lengths $l_{\mathrm{CNT}} = 4 - 20$ μm.

Keywords: random network, carbon nanotubes, thin-film transistor, electrical conductance

1. Introduction

Recently, random carbon nanotube networks have been demonstrated as potential active materials in electronics applications [1], optoelectronics [2], and sensors [3]. Carbon nanotube thin-film transistors are expected to enable the fabrication of high-performance, flexible and transparent devices using relatively simple techniques [4, 5, 6, 7, 8, 9, 10, 11]. As-grown networks of single-walled carbon nanotubes (CNTs) contain both metallic (m-CNTs) and semiconducting (s-CNTs) nanotubes, which leads to a trade-off between on-conductance and on/off conductance ratio [12, 13, 14]. If the density of CNTs in a thin-film transistor (TFT) is sufficiently high that m-CNTs exceed the percolation threshold, the CNT network will become predominantly metallic and, hence, the on/off ratio is very small. In contrast, if the CNT density is so low that a conduction path through the m-CNTs does not exist, a high on/off ratio can be attained, but under such circumstances the low on-conductance is disadvantage [15].

Various experimental efforts have been made in order to increase both on-conductance and on/off ratio of CNT TFTs. With roughly 1/3 as-grown CNTs being metallic, extra steps such as, selective removal of m-CNTs via electrical breakdown method [16], are used in order to cut the metallic paths through the transistors. However, such breakdown also removes some s-CNT pathways leading to significant decrease in the on-conductance. Other authors used semiconducting enriched CNTs in order to enhance the performance of CNT TFTs. For example, methods which separate CNTs by electronic type, such us centrifugation of compositions of CNTs with surface active components in density-gradient media [17] or gas-phase plasma hydrocarbonation reaction technique [18] are used during or after CNTs synthesis process. However, these techniques also create defects in the remaining CNT networks and add impurities, which degrade the overall performance of the TFTs [19, 20, 21]. This adds more difficulties to the fabrication process and the repeatability and uniformity of devices are uncertain [19]. The CNT TFTs are expected to be used in the drivers and logic circuits of future devices, including low-cost, printable e-papers, and radio-frequency identification tags [25]. For such applications, it is advantageous that the functional material for the active layer be deposited on a flexible substrate using a fast, room-temperature, and non-vacuum processing. The effects of m-CNTs in a random network can be reduced by carefully controlling the CNT density, length and device geometry such that the metallic fraction of the CNTs is bellow the percolation threshold [1], i.e., every conducting path contains at least one semiconducting CNT.

An optimized device, i.e., the highest possible on-conductance at a given on/off ratio has the total density of CNTs above the percolation threshold and density of m-CNTs bellow the percolation threshold. Although such high quality devices have been reported in the literature [15, 22, 23, 24], numerical simulations and experiments to determine the CNT density, channel size and CNT length for optimum device performance fabricated at industrial yield rates are lacking.

In this paper, we study the effect of the device parameters (density of CNTs, channel

dimensions and CNT length) on electrical properties in order to obtain optimized and uniform device performance without using any postgrowth treatment. We identify probabilities of different conduction regimes of random CNT network based on our recently determined scaling laws for asymmetric systems of percolating sticks [26]. In this work, we demonstrate how geometrical aspects contribute to feasibility random CNT networks as switches: good transistor performance (i.e., high on-current and on/off ratio) and uniform performance of realized devices.

2. Numerical method

Monte Carlo (MC) simulations are coupled with an efficient iterative algorithm implemented on the grid platform and used to investigate electrical properties of CNT networks [26, 27, 28, 29]. Details on comparison of model with existing experimental data found in literature can be found in Supplementary Information. We consider the two-dimensional systems with isotropically placed CNTs modeled as width-less sticks with a fixed length $l_{\rm CNT}$. The centers of the CNTs are randomly positioned and oriented inside a channel with length $L_{\rm CH}$ and width $W_{\rm CH}$. Source and drain electrodes are placed at the left and right sides of the channel. The top and bottom boundaries of the system are free and nonconducting, because the free boundary conditions are more consistent with the CNT networks in practice. The behavior of the CNT network is studied in terms of the normalized CNT density $n = N/\mathcal{L}^2$, where N is the total number of CNTs and $\mathcal{L} = \sqrt{LW}$ is the normalized channel size, where $L = L_{\rm CH}/l_{\rm CNT}$ is the normalized channel length and $W = W_{\rm CH}/l_{\rm CNT}$ is the normalized channel width, see [30]. The aspect ratio of the system r is defined as the ratio of the channel length and width $r = L/W$, see [26]. Without elaborated postgrowth treatments, CNTs synthesized using any available method are heterogeneous in the sense that they are always a mixture of metallic and semiconducting nanotubes with an approximate ratio of 1:2 [31, 20], i.e., the fraction of the m-CNTs is $f_{\rm M} = 1/3$ and the rest are s-CNTs with fraction $f_{\rm S} = 2/3$ ‡.

We only consider long-channel limits ($L_{\rm CH} > l_{\rm CNT}$) consistent with macroelectronics [12] and low-bias conditions under which nonlinear effects are negligible [31]. For long-channel limits conduction in the CNT network is described by percolation theory as being that of a non-classical two-dimensional conductor [27]. Two sticks (CNTs) belong to the same cluster if they intersect. The system percolates (conducts) if the electrodes (source and drain) are connected with the same cluster [32]. §

The conductance along a CNT segment in on-state $G_{\rm seg}$ is assumed uniform and can be calculated using [23, 24, 33]

$$G_{\rm seg} = \frac{4e^2}{h}\frac{\lambda}{\lambda + l_{\rm seg}}, \tag{1}$$

‡ The CNTs exist as metallic or semiconducting, based on their chirality and composition.

§ The percolation threshold of the infinite-size stick system is defined by the critical density $n_{\rm c} \approx 5.64$ [26]. Similarly, the percolation threshold of only s-CNTs is defined by the critical density $n_{\rm c}/f_{\rm S} \approx 8.46$ and the percolation threshold of only m-CNTs is $n_{\rm c}/f_{\rm M} \approx 16.9$.

where e is the electron charge, h is the Planck's constant, l_{seg} is the length of the CNT segment, and λ is the mean free path of the electrons that is taken as 1.0 μm for m-CNTs and 0.3 μm for s-CNTs [34, 35, 36]. We consider that the conductance of a m-CNT is independent of the gate voltage [31] and in off-state is also given by equation (1). At the same time, we assume that the conductance of a s-CNT in off-state is 10^6 times lower than in on-state, since on/off ratio is usually about 10^6 for well-performing transistors based on individual s-CNTs [37, 38]. Equation (1) assumes diffusive electrical transport through the CNTs typical for the rodlike nanostructures whose length is larger than the mean free path of the electrons ($l_{\text{CNT}} \gg \lambda$). For the diffusive electrical transport the electrical conductance of a stick segment is inversely proportional to the length of the CNT segment $(4e^2/h)(\lambda/l_{\text{seg}})$, cf. [39, 40]. The conductance of the CNT whose length is lower than the mean free path of the electrons ($l_{\text{CNT}} \ll \lambda$) is near the ballistic transport limit $4e^2/h$ and also can be assumed by equation (1), cf. [38, 34].

Internal nodes for contacts between pairs of CNTs are distinguished from boundary nodes for contacts between CNTs and the source/drain electrodes. The contact conductances for the internal nodes are assigned the following values: (i) $0.1e^2/h$ for the junction between two m-CNTs or between two s-CNTs and (ii) 100 times lower conductance for the junction between one m-CNT and one s-CNT, as we neglect the rectifying behavior under low-bias conditions [31, 41]. The contact resistance at the boundary nodes is neglected since electrodes fabricated using, for example, Au [1], Pd [38], or aligned arrays of m-CNTs [42] yield good Ohmic contact to CNTs. Therefore, if a CNT intersects an electrode the potential of the electrode is applied to the intersection point. Kirchhoff's current law was used to balance the current flow through each node of the created network. An iterative equation solver (i.e., conjugate gradient method with Jacobi preconditioner) has been employed to solve a large system of the linear equations following from the Kirchhoff's laws [27]. After obtaining the total source-drain current I under an applied voltage V the macroscopic electrical conductance of the system is evaluated as $G = I/V$, see ‖. Finally, for each set of system parameters, electrical conductances for on- and off-state are calculated for more than 10^5 independent MC realizations for systems with normalized size $L = W = 2$ down to 10^4 realizations for the largest system $L = W = 50$ studied. The results obtained using our conductance model show an excellent agreement with recently published experimental results, see Supplementary Information.

‖ On/off ratio is defined as a ratio of on- and off-current, i.e., $I_{\text{ON}}/I_{\text{OFF}}$, at the same source-drain voltage V applied in on- and off-state. We only consider low-bias conditions, i.e., $V \approx 0$, under which nonlinear effects are negligible and on- and off-currents are given by $I_{\text{ON}} = G_{\text{ON}}V$ and $I_{\text{OFF}} = G_{\text{OFF}}V$, respectively. Therefore, the on/off current ratio $I_{\text{ON}}/I_{\text{OFF}}$ is equal to the on/off conductance ratio, i.e., $G_{\text{ON}}/G_{\text{OFF}}$.

3. Symmetric-channel results

The randomly generated CNT network, if conducting, belongs to one of three complementary CNT network regimes according to their percolation characteristics: (i) neither m-CNT nor s-CNT path exists but the whole network is percolated through a mixed path comprising m- and s-CNTs ($\overline{\mathrm{S}}\overline{\mathrm{M}}$), (ii) only s-CNT paths exist ($\mathrm{S}\overline{\mathrm{M}}$), and (iii) at least one m-CNT path exists (M).

Figure 1 illustrates the structure of the CNT networks and the redistribution of the currents in on- and off-state with increasing the CNT density n. When the CNT density n increases the randomly generated CNT network moves from one operation regime to another. The first regime ($\overline{\mathrm{S}}\overline{\mathrm{M}}$) corresponds to situation when the density of CNTs ($n = 8$) is higher than the percolation threshold of the entire network n_c but lower than the percolation threshold of only s-CNTs ($n_\mathrm{c} < n < n_\mathrm{c}/f_\mathrm{S}$). In this situation the percolation network consists mixed m- and s-CNTs. As a result, the on-conductance G_ON and resulting on-current I_ON are reduced by the presence of the low-conductive s-CNT/m-CNT junctions, see figure 1(a). At the same time, since a m-CNT path does not exist, off-conductance is low and, therefore, on/off ratio is high, cf. figures 1(a) and (b). The second operation regime ($\mathrm{S}\overline{\mathrm{M}}$) occurs for the medium CNT density ($n_\mathrm{c}/f_\mathrm{S} < n < n_\mathrm{c}/f_\mathrm{M}$) when only s-CNT paths exist, and the current flows through high-conductance s-CNT/s-CNT junctions resulting in high on-current I_ON, see figure 1(c). However, CNT density ($n = 12$) is still lower than the percolation threshold of only m-CNTs and the CNT TFT in off-state is not short-circuited through a m-CNT path. Therefore, CNT network can simultaneously achieve high on-conductance G_ON and high on/off ratio $G_\mathrm{ON}/G_\mathrm{OFF}$, cf. figures 1(c) and 1(d). Finally, the third regime (M) of CNT network according to the percolation characteristics occurs at densities close and above the percolation threshold of only m-CNTs, i.e., $n_\mathrm{c}/f_\mathrm{M}$. For high CNT density ($n = 16$) at least one m-CNT path exists and high on-conductance is obtained, see Fig 1(e). On the other hand, in off-state the CNT network is shorted through m-CNTs and, hence, the on/off ratio is very low, cf. figures 1(e) and 1(f). Therefore, CNT network in M operation regime can not be used as an active media for transistors with a high switching performance.

We will determine region of CNT density n where s-CNT paths are dominant($\mathrm{S}\overline{\mathrm{M}}$) based on our recently determined parameters for moments of percolation probability distribution. In this region on-current and on/off ratio are expected to be high ¶. We define a density range with lower $n_{L,R}^{\mathrm{low}}$ and upper boundary $n_{L,R}^{\mathrm{high}}$, where probability of percolation only through s-CNT paths ($\mathrm{S}\overline{\mathrm{M}}$) is higher then R ($0 \leq R \leq 1$). As one would expect, the range defined by $n_{L,R}^{\mathrm{high}}$ and $n_{L,R}^{\mathrm{low}}$ increases with the normalized system size L and decreases with R, cf. figure 2. We can further observe interesting features of the shape of the $\mathrm{S}\overline{\mathrm{M}}$ percolation density range with increasing the system size: (i) the position of $\mathrm{S}\overline{\mathrm{M}}$ percolation probability maximum n_L^{max} converges to $2n_\mathrm{c}$ with increasing the system size, (ii) low-bound density $n_{L,R}^{\mathrm{low}}$ decreases and converges to the

¶ Details of analytic model are given in Supplementary Information.

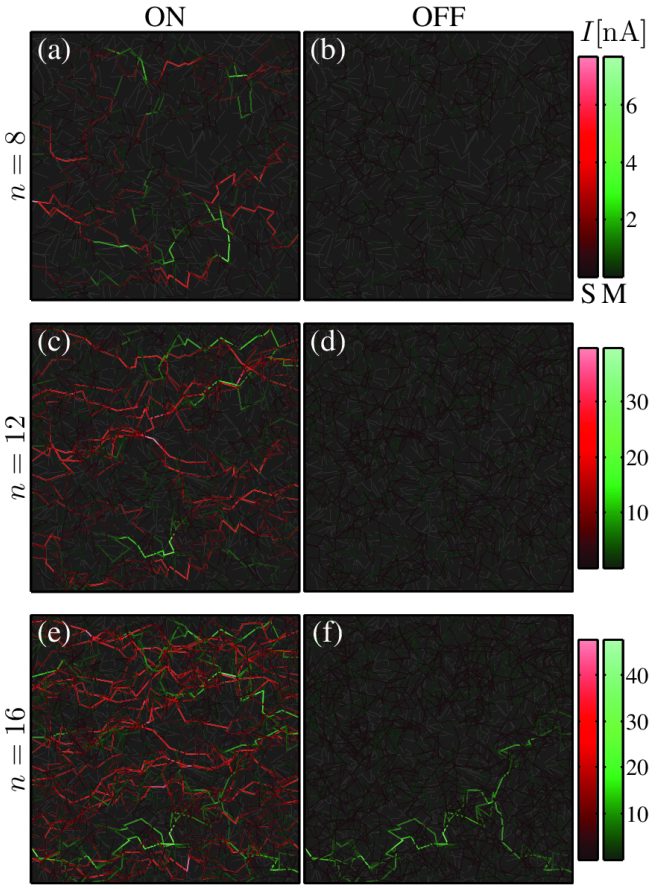

Figure 1. Simulated on- (a), (c), and (e) and off-current (b), (d), and (f) distribution for different CNT densities. The source-drain voltage is $V = 0.1$ V, CNT length is $l_{\mathrm{CNT}} = 5$ μm, and channel dimensions are $L_{\mathrm{CH}} = W_{\mathrm{CH}} = 50$ μm, i.e., the normalized system size is $L = 10$. (a) When the density of CNTs ($n = 8$) is significantly lower than the percolation threshold of only s-CNTs ($n < n_{\mathrm{c}}/f_{\mathrm{S}}$) the dominant percolation domain is through mixed paths comprising m- and s-CNTs ($\overline{\mathrm{S}}\overline{\mathrm{M}}$). (b) Since there is no percolating path through only m-CNTs the off-current is low, i.e., the on/off ratio is high. (c) For higher CNT density ($n = 12$) only s-CNT paths exist ($\mathrm{S}\overline{\mathrm{M}}$) resulting in a high on-current I_{ON}. (d) CNT density is still lower than the percolation threshold of only m-CNTs and therefore, the CNT TFT is not short-circuited in off-state and on/off ratio is still high. (e) For high CNT density ($n = 16$) m-CNT network percolates. (f) The CNT network in off-state is shorted through the m-CNTs.

percolation threshold of s-CNT paths $n_{\mathrm{c}}/f_{\mathrm{S}}$, and (iii) high-bound density $n_{L,R}^{\mathrm{high}}$ increases and converges to the percolation threshold of m-CNT paths $n_{\mathrm{c}}/f_{\mathrm{M}}$, see figure 2.

In the rest of this section, we will quantify the dependence of calculated on-conductance and on/off ratio on the CNT density, length, and system size. Our aim is further to restrict parameter range for which acceptable transistor characteristics are obtained with a realisation probability higher than 99%. For most kinds of integrated circuit applications acceptable values for on-conductance and on/off ratio are 1 μS and 10^4, respectively [20, 35, 43].

The results are shown in figure 3 as a function of the CNT normalized density n for

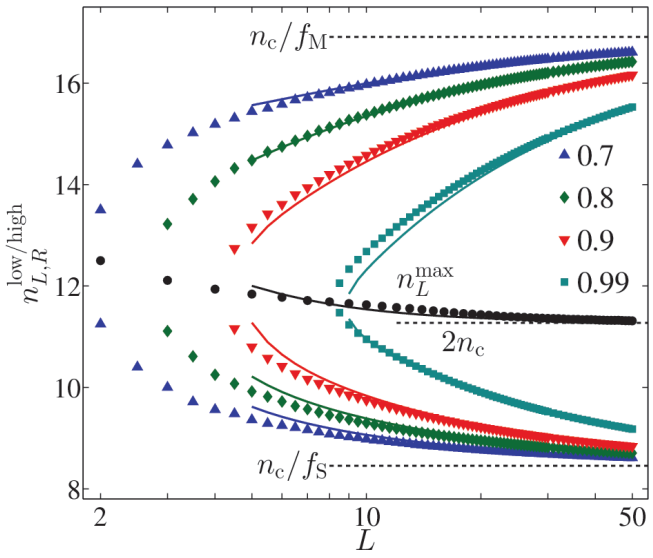

Figure 2. The dependence of $S\overline{M}$-dominant region on the normalized system size L, for different tolerances $R = 0.7, 0.8, 0.9$, and 0.99. The points are the MC simulation results and the solid lines are obtained using analytic model (see Supplementary Information). With increasing the system size L, value of CNT density n_L^{max}, where percolation probability only through s-CNT paths $R_{n,L}^{S\overline{M}}$ reaches maximum, converges to $2n_c$, low-bound density $n_{L,R}^{low}$ to n_c/f_S, and high-bound density $n_{L,R}^{high}$ to n_c/f_M.

$l_{CNT} = 5\ \mu$m and the system size $W_{CH} = L_{CH} = 100\ \mu$m, i.e., the normalized system size $L = 20$. The on-conductance G_{ON} increases with CNT density n and the 1st and 99th percentiles converge to the median value, see figure 3(a). The difference between the 99th and 1st percentile of the on/off ratio G_{ON}/G_{OFF} reaches minimum close to n_{20}^{max} and rapidly increases when the CNT density n becomes higher than $n_{20,0.99}^{high}$, see figure 3(b). For densities higher than $n_{20,0.99}^{high}$ the percolation probability of M configurations $R_{n,L}^{M}$ is higher than 1%, i.e., $R_{n,L}^{M} > 1\%$ and therefore, the 1st percentile realization belongs to the M regime and the sharp decrease in on/off behavior is obtained. One can observe that maximum of on/off ratio is between the densities $n_{20,0.99}^{low}$ and $n_{20,0.99}^{high}$. More than 99% of realized devices exhibit simultaneously on-conductance higher than 1 μS and on/off ratio higher than 10^4 when the normalized density n is close to n_{20}^{max}, cf. figures 3(a) and 3(b).

A similar behavior of the on-conductance G_{ON} and the on/off ratio G_{ON}/G_{OFF} can be observed in figure 4(a) with increasing the normalized system size L. While the percentiles of the on-conductance G_{ON} experience continuous convergence to the infinite system value, the on/off ratio exhibits a sharp transition in the 1st percentile behavior at the normalized system size $L \approx 7$. For the system size bellow $L < 7$ the percolation probability of realizations through only m-CNTs is higher than 1%, i.e., $R_{n,L}^{M} > 1\%$ and therefore, the 1st percentile realization is short-circuited with $G_{ON}/G_{OFF} < 10$, cf. Supplementary Information for probability distribution functions of on/off ratio. On the other hand, more than 99% of realized devices exhibit simultaneously on-conductance higher than 1 μS and on/off ratio higher than 10^4 when the normalized system size is

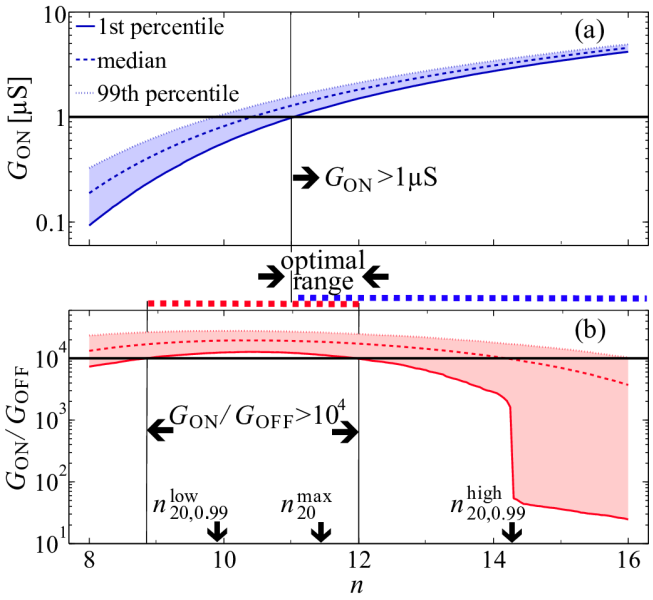

Figure 3. On-conductance G_{ON} (a) and on/off ratio G_{ON}/G_{OFF} (b) as a function of the normalized CNT density n for symmetric TFT with the CNT length $l_{CNT} = 5$ μm and channel size $L_{CH} = W_{CH} = 100$ μm, i.e., the normalized system size $L = 20$. Solid line represents the 1st percentile, while the dashed and dotted lines correspond to the median and 99th percentile, respectively, of the device population. The arrows denote regions where more than 99% of devices have: (a) on-conductance higher than 1 μS (horizontal bold line) or (b) on/off ratio higher than 10^4 (horizontal bold line). The positions of lower $n^{low}_{20,0.99}$ and higher $n^{high}_{20,0.99}$ bounds of 0.99 percolation probability for S$\overline{\text{M}}$ regime are also given, as well as position of S$\overline{\text{M}}$ probability maximum $n^{max}_{8,50}$.

$L > 16$, see figure 4(a).

The influence of CNT length l_{CNT} on the transistor performance is explored in figure 4(b). Here, the normalized system size is fixed and large $L = 20$, in order to minimize influence of finite-size scaling effects on the transistor performance, see also **??**. Therefore, on-conductance G_{ON} and on/off ratio G_{ON}/G_{OFF} depend only on the electrical characteristics of the nanotubes, i.e., their length l_{CNT}, in accordance with equation (1). When the CNT length l_{CNT} is larger than the electron mean free path, i.e., $l_{CNT} > 1$ μm, diffusive transport in CNTs becomes dominant and the on-conductance G_{ON} of the network starts to decrease linearly with the CNT length, see figure 4(b). At the same time, due to a increased resistance of m-CNTs, leak-currents in off-state through the m-CNTs decrease and on/off ratio improves with increasing the CNT length, see figure 4(b). It is important to note that in this trade-off, the improvement of on/off ratio is one order of magnitude with increasing l_{CNT} from 1 μm to 10 μm while G_{ON} decreases only 10%. However, more than 99% of realized devices exhibit simultaneously high on-conductance and high on/off ratio when the CNT length is between $l_{CNT} = 4 - 12$ μm, cf. figures 4(b).

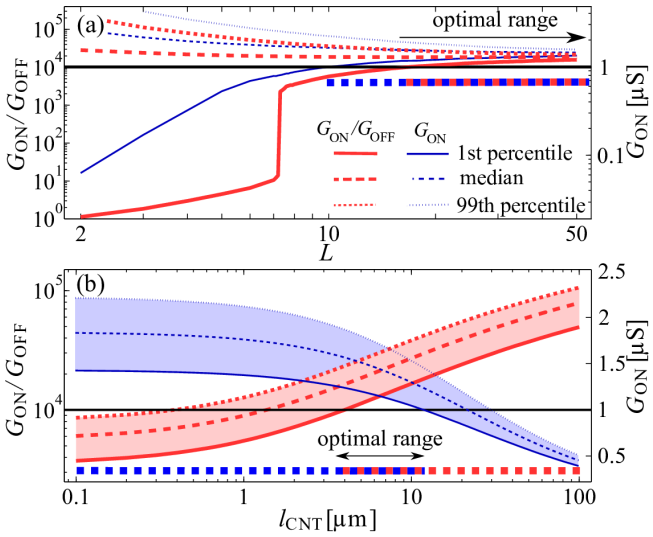

Figure 4. The dependence of on-conductance $G_{\rm ON}$ and on/off ratio $G_{\rm ON}/G_{\rm OFF}$ on (a) normalized system size L for symmetric-channel TFTs with CNT length $l_{\rm CNT} = 5$ μm and normalized density $n_L^{\rm max}$ and (b) CNT length $l_{\rm CNT}$ for symmetric system with the normalized size $L = 20$ and the normalized CNT density n equal to $n_{20}^{\rm max} = 11.45$. Solid line represents the 1st percentile, while the dashed and dotted lines correspond to the median and 99th percentile, respectively, of the device population. The arrows denote regions where more than 99% of devices have on-conductance higher than 1 μS and on/off ratio higher than 10^4 (horizontal bold line).

4. Asymmetric-channel results

For the case of the asymmetric channel the dependence of the normalized density $n_{L,W}^{\rm max}$ where $\overline{\rm SM}$ percolation probability reaches maximum on the normalized system dimensions L and W is shown in Fig 5(a). The normalized density $n_{L,W}^{\rm max}$ increases with increasing the normalized channel length L and decreases with increasing the width W, cf. 5(a) and Supplementary Information. The agreement between the MC simulation results $n_{L,W}^{\rm max}$ and the values $n_{L,W}^{\rm model}$ obtained from our analytic model (cf. Supplementary Information) is better than 9% for the systems with $L > 5$, see figure 5(b). From figures 5(c) and 5(d) we expect to achieve 99% of only s-CNTs conducting realizations roughly above the line $L_{\rm CH}W_{\rm CH} > 250\ l_{\rm CNT}^2$. Within that region we see that $n_{L,W,0.99}^{\rm low}$ depends only on the system width W. On the other hand, the upper limit of 99% confidence region, $n_{L,W,0.99}^{\rm high}$ depends on both the normalized length L and width W.

The random CNT TFTs with an asymmetric channel have similar characteristics of the on-conductance $G_{\rm ON}$ and on/off ratio $G_{\rm ON}/G_{\rm OFF}$ compared to the symmetric-channel configurations, cf. figures 3 and 6. The on-conductance $G_{\rm ON}$ also increases with increasing the CNT density n and the 1st and 99th percentiles converge to the median value, see figure 6(a). The difference between the 99th and 1st percentile of on/off ratio $G_{\rm ON}/G_{\rm OFF}$ also reaches minimum close to the density where probability of $\overline{\rm SM}$ percolation reaches maximum, i.e., $n_{8,50}^{\rm max}$, and rapidly increases when the CNT density becomes higher than $n_{8,50,0.99}^{\rm high}$, see figure 6(b). Similarly, the maximum of the

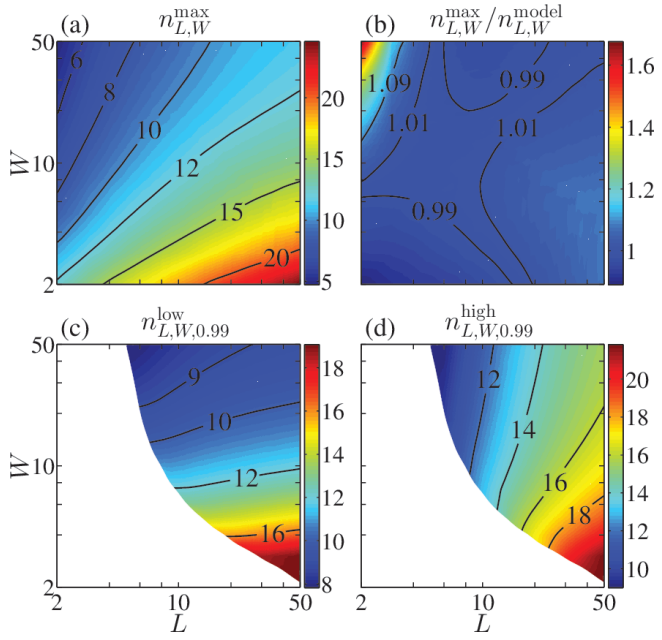

Figure 5. The dependence of (a) the normalized density $n^{\max}_{L,W}$ where the probability of S$\overline{\text{M}}$ percolation reaches maximum and (b) the ratio between the MC simulation results $n^{\max}_{L,W}$ and the values $n^{\text{model}}_{L,W}$ are obtained using analytic model (cf., Supplementary Information) on the normalized channel width W and length L . The low-bound $n^{\text{low}}_{L,W,0.99}$ (c) and high-bound density $n^{\text{high}}_{L,W,0.99}$ (d) determine a density range where the probability of S$\overline{\text{M}}$ realizations is higher than 0.99.

on/off ratio is between densities $n^{\text{low}}_{8,50,0.99}$ and $n^{\text{high}}_{8,50,0.99}$, and more than 99% of realized devices exhibit simultaneously on-conductance higher than 1 μS and on/off ratio higher than 10^4 when the normalized density n is close to $n^{\max}_{8,50}$, cf. figures 6(a) and 6(b). Hence, the density $n^{\max}_{L,W}$ for an asymmetric, as well as symmetric, configurations can be used as a compromise value for obtaining the optimized transistor performance, see figures 3 and 6. However, the narrow-channel configurations generally have a higher on-conductance compared to the symmetric channels (see Supplementary Information). Indeed, as can be seen from figures 3(a) and 6(a), narrow-channel TFT with the aspect ratio $r = 8/50$ has roughly $1/r \approx 6$ times higher on-conductance G_{ON} compared to the symmetric-channel configuration with the same normalized channel size $\mathcal{L} = 20$ and CNT length $l_{\text{CNT}} = 5$ μm.

The 1st percentiles of the on-conductance G_{ON} and on/off ratio $G_{\text{ON}}/G_{\text{OFF}}$ are calculated for the same structural parameters L, W, and $n^{\max}_{L,W}$, and different CNT lengths $l_{\text{CNT}} = 4, 8, 12$ μm, see figure 7. In accordance to the results shown for the symmetric-channel configuration in figure 4(b) we note that with increasing the CNT length l_{CNT} the on-conductance G_{ON} decreases, while the on/off ratio $G_{\text{ON}}/G_{\text{OFF}}$ increases, see figure 7. When the CNT length l_{CNT} is bellow 4 μm ballistic electrical transport becomes dominant and the on/off ratio becomes lower than 10^4, cf. figures 7(b), 7(d), and 7(f). On the other hand, when l_{CNT} is higher than 20 μm a high on-conductance can be attained only for a very large channel with dimensions of the order

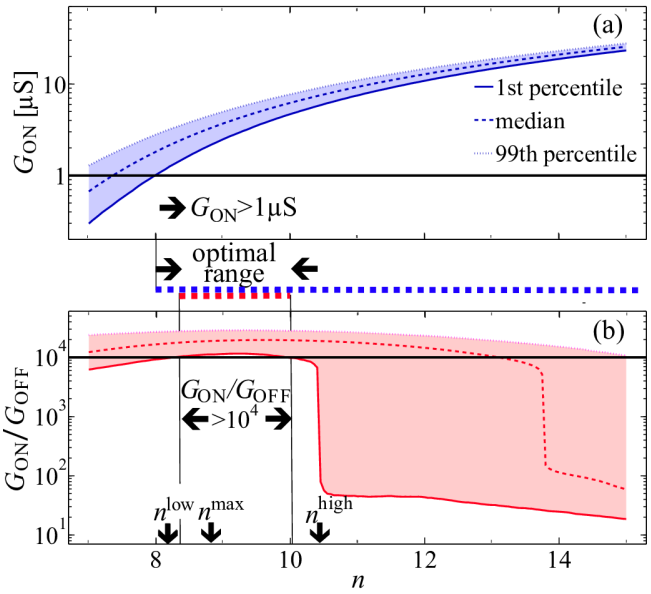

Figure 6. On-conductance G_{ON} (a) and on/off ratio G_{ON}/G_{OFF} (b) as a function of the normalized CNT density n for narrow-channel TFT with $l_{CNT} = 5$ μm and the channel dimensions $L_{CH} = 40$ μm and $W_{CH} = 250$ μm, i.e., the normalized system dimensions $L = 8$ and $W = 50$. Solid line represents the 1st percentile, while the dashed and dotted lines correspond to the median and 99th percentile, respectively, of the device population. The arrows denote regions where more than 99% of devices have: (a) on-conductance higher than 1 μS (horizontal bold line) or (b) on/off ratio higher than 10^4 (horizontal bold line). The positions of lower $n^{low}_{8,50,0.99}$ and higher $n^{high}_{8,50,0.99}$ bounds of 0.99 percolation probability for S$\overline{\text{M}}$ regime are also given, as well as position of S$\overline{\text{M}}$ probability maximum $n^{max}_{8,50}$.

of 1 mm, see figure 7(e). Hence, the CNT length in the range $l_{CNT} = 4 - 20$ μm results in an acceptable balance between the on-conductance and on/off performance of the CNT TFTs.

Regions A and B in figure 7 represent the CNT networks with a low 1st-percentile value of the on-conductance G_{ON}. The region A is defined as a region where the probability of $\overline{\text{S}}\overline{\text{M}}$ percolation is higher than 1%, i.e., $R^{\overline{\text{S}}\overline{\text{M}}}_{n,L,W} > 1\%$ and therefore, the 1st-percentile realization is mixed path with low-conductive s-CNT/m-CNT junctions. The realizations in the region B have a high value of the aspect ratio r and therefore, a low overall on-conductance (see Supplementary Information). On the other hand, regions C and D in figure 7 represent the CNT networks with a low 1st-percentile value of the on/off ratio G_{ON}/G_{OFF}. The TFTs in the region C feature networks with the probability of percolation through only m-CNTs higher than 1%, i.e., $R^{M}_{n,L,W} > 1\%$ and therefore, the 1st-percentile realization is short-circuited having a very low G_{ON}/G_{OFF}. The networks operating in D region are not short-circuited but the on/off ratio is low because of high leak-currents in off-state through the high-density m-CNTs. We can conclude that optimal dimensions of CNT TFT channel regarding to the device switching performance are those outside the regions A, B, C, and D shown in figure 7. The dotted

lines approximate the region where CNT TFTs attain high on-conductance and at the same time high on/off ratio. Therefore, the random CNT TFTs with the channel aspect ratio $L_{\rm CH}/W_{\rm CH} < 1.2$ and the normalized size $L_{\rm CH}W_{\rm CH}/l_{\rm CNT}^2 > 250$ with a probability higher than 99% exhibit on-conductance higher than 1 μS and at the same time on/off ratio higher than 10^4.

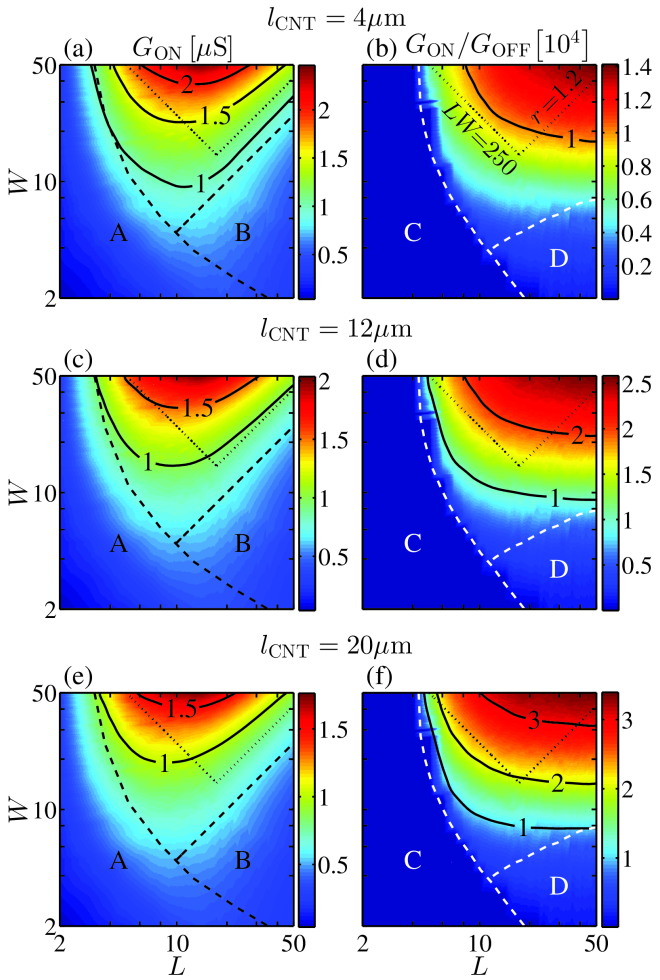

Figure 7. The results for the 1st percentile of the on-conductance $G_{\rm ON}$ (a), (c), and (e) and on/off ratio $G_{\rm ON}/G_{\rm OFF}$ (b), (d), and (f) calculated at $n_{L,W}^{\rm max}$ as a function of the normalized channel width W and length L for different CNT lengths $l_{\rm CNT} = 4, 12, 20$ μm. The region A represents CNT TFT configurations with the probability of $\overline{\rm S}\overline{\rm M}$ percolation higher than 1%, i.e., $R_{n,L,W}^{\overline{\rm S}\overline{\rm M}} > 1\%$, while the region B represents configurations with a high aspect ratio (here $r > 2$). TFTs in the C region feature networks with the probability of M percolation higher than 1%, i.e., $R_{n,L,W}^{\rm M} > 1\%$, while the region D denotes networks with a high CNT density (here $n > 15$). The area above the dotted lines ($LW = 250$ and $L/W = 1.2$) can be used as an approximation of the region where the random CNT TFTs simultaneously attain high on-conductance and high on/off ratio.

5. Conclusions

In this paper, we present the numerical simulation results of switching performance of the transistors based on random networks of as-grown CNTs. The CNT thin films studied here are viewed as a material for the low-cost, flexible, and transparent field-effect transistors. A factor that makes CNT films complex is that they contain both metallic and semiconducting nanotubes. Only the s-CNTs have highly modulated conductance by the gate and only junctions between CNTs of the same type are highly conductive. Therefore, the random CNT TFTs that percolate only through s-CNT paths can simultaneously attain high on-conductance and high on/off ratio. As a result, a key limitation in scaling-up production of the random CNT TFTs with high on-current and on/off ratio is a requirement to achieve uniform performance of the realized devices.

We demonstrate utility of the percolation probability functions for as-grown CNT networks. The derived expressions for the percolation probability functions represent an excellent fit to the data calculated using simulations. We also show that the fraction of 1:2 of metallic to semiconducting nanotubes provides a sufficient design freedom. We avoid creating m-CNT paths, while at the same time determine a density range where the rate of realizations that percolate only through s-CNT paths is higher than 99%. Since there is a trade-off between the on-conductance and on/off ratio regarding to the CNT density we show that the position of only s-CNT percolation probability maximum can be used as a good balance for the CNT density value. We have included into the CNT conductance model diffusive electrical transport through the CNTs typical for the rodlike nanostructures whose length is larger than the mean free path of the electrons. This enabled us to consider influence of the CNT length on the device characteristics. When the CNT length increases diffusive transport in the CNTs becomes dominant and on-conductance decreases with the CNT length. At the same time, because of increased resistance of m-CNTs, the leak-currents in off-state through the m-CNTs decrease and on/off ratio improves. This results in a further trade off, still the improvement of the on/off ratio is much larger than detrimental loss of the on-conductance.

The asymmetric systems have smaller finite-size scaling exponents than symmetric. This results in more pronounced finite-size scaling behavior than in symmetric case and enables us even more design freedom. We conclude that decrease of the channel length is a good strategy for the performance improvement for two reasons: (i) the on-conductance increases with decreasing the aspect ratio and (ii) the percolation only through s-CNT paths occurs at lower densities resulting in the lower costs of TFT production. Following this, we have performed a parameter study to find optimal channel dimensions for CNT TFTs. We present a region of the channel dimension where the most of the random CNT realizations have satisfactory transistor performance. According to the criteria of a high on-conductance and at the same time a high on/off ratio, within 99% confidence range, the optimal region of channel dimensions can be estimated with aspect ratio $L_{\mathrm{CH}}/W_{\mathrm{CH}} < 1.2$ and size $L_{\mathrm{CH}}W_{\mathrm{CH}}/l_{\mathrm{CNT}}^2 > 250$. This conclusion remains valid when the CNT length belongs to the range $l_{\mathrm{CNT}} = 4 - 20$ μm

resulting in an acceptable balance between the on-conductance and on/off performance of the random CNT TFTs. At the end, we have demonstrated that results of our model for on-conductance and on/off ratio show an excellent agreement with the recently published experimental results. Hence, we conclude that the channel dimensions L_{CH} and W_{CH}, CNT length l_{CNT}, and density n are the only parameters needed for description and optimization of TFTs based on random networks of as-grown CNTs.

Acknowledgments

This work was supported by the Ministry of Education, Science, and Technological Development of the Republic of Serbia under project ON171017, OI1611005, and OI1611003, es well as, by the European Commission under H2020 project DAFNEOX, Grant No. 645658. Numerical simulations were run on the PARADOX supercomputing facility at the Scientific Computing Laboratory of the Institute of Physics Belgrade.

References

[1] Cao Q, Kim H-S, Pimparkar N, Kulkarni J P, Wang C, Shim M, Roy K, Alam M A and Rogers J A 2008 *Nature* **454** 495
[2] De Volder M F L, Tawfick S H, Baughman R H and Hart A J 2013 *Science* **339** 535
[3] Abdelhalim A, Abdellah A, Scarpa G and Lugli P 2014 *Nanotechnology* **25** 055208
[4] Engel M, Small J P, Steiner M, Freitag M, Green A A, Hersam M C and Avouris P 2008 *ACS Nano* **2** 2445
[5] Sun D-M, Timmermans M Y, Tian Y, Nasibulin A G, Kauppinen E I, Kishimoto S, Mizutani T and Ohno Y 2011 Nat. Nanotechnol. **6** 156
[6] Chandra B, Park H, Maarouf A, Martyna G J and Tulevski G S 2011 *Appl. Phys. Lett.* **99** 072110
[7] Wang C, Chien J-C, Takei K, Takahashi T, Nah J, Niknejad A M and Javey A 2012 *Nano Lett.* **12** 1527
[8] Park S, Vosguerichian M and Bao Z 2013 *Nanoscale* **5** 1727
[9] Lau P H, Takei K, Wang C, Ju Y, Kim J, Yu Z, Takahashi T, Cho G and Javey A 2013 *Nano Lett.* **13** 3864
[10] Liu N, Yun K N, Yu H-Y, Shim J H and Lee C J 2015 *Appl. Phys. Lett.* **106** 103106
[11] Li J and Pandey G P 2015 *Annu. Rev. Phys. Chem.* **66** 331
[12] Kumar S, Pimparkar N, Murthy J Y and Alam M A 2006 *Appl. Phys. Lett.* **88** 123505
[13] Kocabas C, Pimparkar N, Yesilyurt O, Kang S J, Alam M A and Rogers J A 2007 *Nano Lett.* **7** 1195
[14] Rouhi N, Jain D and Burke P J 2011 ACS Nano **5** 8471
[15] Sangwan V K, Behnam A, Ballarotto V W, Fuhrer M S, Ural A and Wiliams E D 2010 *Appl. Phys. Lett.* **97** 043111
[16] Collins P G, Arnold M S and Avouris P 2001 *Science* **292** 706
[17] Arnold M S, Green A A, Hulvat J F, Stupp S I and Hersam M C 2006 *Nat. Nanotechnol.* **1** 60
[18] Zhang G, Qi P, Wang X, Lu Y, Li X, Tu R, Bangsaruntip S, Mann D, Zhang L and Dai H 2006 *Science* **314** 974
[19] Kumar S, Cola B A, Jackson R and Graham S 2011 *J. Elect. Packaging* **133** 020906
[20] Hu L, Hecht D S and Grüner G 2010 *Chem. Rev.* **110** 5790
[21] Hecht D S, Hu L and Irvin G 2011 *Adv. Mater.* **23** 1482
[22] Snow E S, Novak J P, Campbell P M and Park D 2003 *Appl. Phys. Lett.* **82** 2145
[23] Li J, Zhang Z-B and Zhang S-L 2007 *Appl. Phys. Lett.* **91** 253127

[24] Seppälä S, Häkkinen E, Alava M J, Ermolov V and Seppälä E T 2010 *Europhys. Lett.* **91** 47002
[25] Che Y, Chen H, Gui H, Liu J, Liu B and Zhou C 2014 *Semicond. Sci. Technol.* **29** 073001
[26] Žeželj M, Stanković I and Belić A 2012 *Phys. Rev.* E **85** 021101
[27] Žeželj M and Stanković I 2012 *Phys. Rev.* B **86** 134202
[28] Stanković I, Kröger M and Hess S 2002 *Comp. Physics Comm.* **145** 371
[29] Balaž A, Vidanović I, Stojiljković D, Vudragović D, Belić A and Bogojević A 2012 *Commun. Comput. Phys.* **11** 739
[30] Heitz J, Leroy Y, Hébrard L and Lallement C 2011 *Nanotechnology* **22** 345703
[31] Fuhrer M S, Nygård J, Shih L, Forero M, Yoon Y G, Mazzoni M S C, Choi H J, Ihm J, Louie S G, Zettl A and McEuen P L 2000 *Science* **288** 494
[32] Stauffer D and Aharony A 2003 *Introduction to Percolation Theory* 2nd revised ed. (London: Taylor and Francis)
[33] Behnam A and Ural A 2007 *Phys. Rev.* B **75** 125432
[34] Javey A, Guo J, Paulsson M, Wang Q, Mann D, Lundstrom M and Dai H 2004 *Phys. Rev. Lett.* **92** 106804
[35] Avouris P 2004 *MRS Bull.* **29** 403
[36] Purewal M S, Hong B H, Ravi A, Chandra B, Hone J and Kim P 2007 *Phys. Rev. Lett.* **98** 186808
[37] Bachtold A, Hadley P, Nakanishi T and Dekker C 2001 *Science* **294** 1317
[38] Javey A, Guo J, Wang Q, Lundstrom M and Dai H 2003 *Nature* **424** 654
[39] Park J-Y, Rosenblatt S, Yaish Y, Sazonova V, Üstünel H, Braig S, Arias T A, Brouwer P W and McEuen P L 2004 *Nano Lett.* **4** 517
[40] Franklin A D and Chen Z 2010 *Nat. Nanotechnol.* **5** 858
[41] Buldum A and Lu J P 2001 *Phys. Rev.* B **63** 161403
[42] Sarker B K, Kang N and Khondaker S I 2014 *Nanoscale* **6** 4896
[43] Wang C, Zhang J and Zhou C 2010 *ACS Nano* **4** 7123
[44] Kuwahara Y, Nihey F, Ohmori S and Saito T 2015 *Carbon* **91**, 370.